Silver Tarnishing Mechanism Revealed by Molecular Dynamics Simulations

Gabriele Saleh[a,b,*], Chen Xu[c] and Stefano Sanvito[a]

[a] School of Physics, AMBER and CRANN institute, Trinity College Dublin, College Green, Dublin 2, Ireland. E-mail: gabrielesaleh@outlook.com

[b] Istituto Italiano di Tecnologia, Via Morego 30, Genova, Italy

[c] Nokia Bell Labs, 600 Mountain Avenue, Murray Hill, NJ, USA

Abstract:

The mechanism of silver-oxygen and silver-sulphur reactions is revealed by means of molecular dynamics simulations, performed with reactive force fields purposely built and extensively tested against quantum chemical results. Different reaction mechanisms and rates for Ag-O and Ag-S emerge. This study solves the long-lasting question as to why silver exposed to the environment is strongly vulnerable to sulphur corrosion (tarnishing) but hardly reacts with O_2, despite thermodynamics predicts both oxide and sulphide to form. The reliability of the simulations results is confirmed by the agreement with a multitude of experimental results from literature.

Silver has been used in art and jewellery for millennia, and it is nowadays ubiquitously adopted for technologically important devices in catalysts[1], electric equipment[2], and localized surface plasmon nanochips[3]. These applications share a common problem: silver corrosion, whose early stage is called 'tarnishing'. Ag corrosion is critical in the electronics industry[2-4], since Ag is used in Printed Circuit Boards (PCBs) as finish material and both to build electronic components and to assemble them on to PCBs. As PCBs are employed in open-air applications, Ag corrosion-related failures are not uncommon[4], and represent an economic burden as well as a performance and reliability issue.

Reduced sulphur compounds such as H_2S, and S_8 are very effective in tarnishing silver, even at part-per-billion (ppb) concentrations[5]. In contrast, O_2 does not form appreciable corrosion products under normal conditions[6]. Note that water is not necessary for tarnishing, although humidity can speed up the reaction[7]. This suggests that Ag tarnishing proceeds through direct chemical reaction rather than through an electrochemical process. Although Ag_2S is the dominant corrosion product in the environments where sulphur is present[8], the formation of silver oxide is occasionally observed and it is attributed to the presence of ozone[6,8]. Considering that even in so-called sulphur-rich environments the O_2 concentration is about 10^9 times larger than that of sulphur, a strong disparity between the reactivity of oxygen and sulphur towards silver emerges. Thermodynamically both Ag_2S and Ag_2O are expected to form under normal p, T conditions[9]. Their formation enthalpies are almost identical, although the entropic factor favour (disfavour) the suphidation (oxidation)[9]. The chemisorption energies of O_2 and S_8 onto Ag(111) surface are very similar as well[10]. It is thus obvious that Ag tarnishing is driven by the dynamics of the Ag-S and Ag-O reactions, the study of which triggered the investigation presented here.

While experiments can observe corrosion at the nanometric scale[11], only computational approaches grant access to the atomistic and electronic details necessary for designing corrosion-resistant materials. Molecular Dynamics (MD) simulations represent the ideal tool to shed light on the silver tarnishing mechanism. ReaxFF[12,13] reactive force fields (*vide infra*) allow fast energy evaluation, hence they can simulate the large dimensions and time scales required for studying corrosion processes. Indeed, corrosion-related reactions were already studied through ReaxFF (*e.g*. refs. 14, 15).

In this work, we unveil the atomic-level Ag/S and Ag/O reaction mechanisms through ReaxFF MD. We simulated a silver slab in contact with gaseous sulphur (S_8) or oxygen (O_2 or O_2-O_3 mixtures). Ag(111) and Ag(001) surfaces were considered, both without and with defects, namely vacancies, adatoms, surface steps and grain boundaries (structures details in Sect. S1.2.2). Throughout this investigation, we tackle the following questions: i) what are the formation mechanisms of silver oxide and sulphide?, and ii) why is sulphur so much more effective than oxygen in tarnishing silver? To do that, we first explore if and how it is possible to generate ReaxFF force fields that are accurate enough to make reliable predictions of corrosion mechanisms.

ReaxFF expresses the energy of *any* system in its electronics ground state as a function of the atomic coordinates through empirical, computationally inexpensive, formulae that depend on certain parameters. These are chosen to best reproduce (in the least-square sense) a given dataset, generally produced through *ab initio* calculations. Our dataset (Training Set - TS) is built from a collection of structures representative of the chemical interactions and of the reaction events that are expected to

occur. TS adopted for previous studies of solid-fluid reactions typically contained the change in energy along some atomic deformations, such as volume-energy curves for solids and bond breaking/formation for molecules. Formation energies and equilibrium lattice constants are often included as well. One then tacitly assumes that, if reaxFF can reproduce the TS data with reasonable accuracy, the same accuracy will be maintained throughout the molecular dynamics simulations. The results of the present study show that such an assumption is not generally true, certainly not for the Ag-S and Ag-O systems.

A detailed description of our ReaxFF fitting procedure can be found in Sect. S2, while here we report the most relevant findings. An initial TS was built by including DFT energy-volume curves for allotropes/polymorphs of Ag and its oxide/sulphide, bond dissociation curves and various deformations of O_n (n=2,3) and S_n (n=2,7,8,10,14, ∞) molecules, Ag surface energies, O/S chemisorption energies on Ag surfaces, and long-range van der Waals interactions for S_n-S_n, O_n-O_n, Ag-O_n, and Ag-S_n . Additionally, unphysical behaviours in the MD simulations (see Sect. S2) are avoided by including in the TS the dissociation curves of O_2 and S_2 onto the Ag(111) surface. Once a good DFT-ReaxFF agreement on the TS was reached, we performed MD simulations on small systems of up to 48 atoms. The ReaxFF-DFT agreement on the energy variation during the simulation, necessary for reliably reproducing the dynamics of the reaction, turned out to be very poor (Fig. S1). Seeking to improve on that, we included in the TS the energy differences among snapshots of the above-mentioned simulations and fit again. The resulting force field was then used for a second MD test simulation, and the procedure was repeated iteratively until no further improvement on the ReaxFF accuracy was possible. Finally, the TS was enriched with those reaction events important for the tarnishing process, namely defects formation energies of Ag, and more dissociation paths of sulphur and oxygen onto Ag surfaces. The final force fields were able to quantitatively reproduce the DFT energy change along the MD simulations for almost every snapshot (Figs S7 and S14). A further confirmation of the reliability of our force field comes from the low average ReaxFF-DFT discrepancy for MD runs that were not included in the fitting. These errors come to 0.95 and 0.56 kcal mol^{-1} $atom^{-1}$ for the Ag-S and Ag-O force fields, respectively. Our results demonstrate that, for solid-gas reactions, ReaxFF cannot be assumed to accurately reproduce reaction events not included in the TS. Therefore, the force field fitting strategy commonly adopted in literature should be reconsidered.

An important difference between Ag-O and Ag-S reactions emerged already when building the TS. The dissociation curve of O_2 onto Ag is characterized by an energy barrier absent for S_2 (Fig. 1). Moreover, the chemisorption well is significantly deeper for sulphur. This is due to the higher repulsion between the two chemisorbed O atoms, discussed below. Note that the presence of a dissociation barrier for O_2 onto Ag had been inferred previously from experimental data[16]. The exact height of the barrier depends on the particular dissociation path followed by the molecule, but our force field is able to reproduce the height for the path included in the TS. The different dissociation behaviour is an important factor for understanding the differences in reactivity between O and S against silver.

[Figure 1]

Concerning the mechanism for silver sulphidation, let us first consider our MD simulations on ordered surfaces. Ag(111) is found to be less reactive than Ag(001) (Fig. S16), in agreement with its more close

packed and hence more stable structure[17]. Ag(001) can serve as a representative example to identify the sulphidation mechanism, which can be understood by closely inspecting the MD trajectories (Fig. 2a). First S_8 molecules physisorb on the surface, then they progressively dissociate into fragments, eventually resulting in chemisorbed S atoms. After about 1 ns, we observe that a number of Ag atoms have moved from the topmost surface layer to adatom positions, and the vacancies thereby created are filled by S atoms (Fig. S18). This represents the crucial feature of Ag sulphidation, which is illustrated in Fig. 2a (right). In the surface regions with a high S coverage (~ 1 ML), Ag atoms tend to move from the (surface) lattice sites to adatom positions surrounded by S atoms. This leaves an Ag vacancy behind, which is then quickly (0.5-5 ps) filled by one of the S atoms present on the surface. We estimated the energetics of these types of events by means of DFT calculations (Fig. 3a). The formation of a vacancy/adatom pair is clearly endothermic on the bare surface, but becomes more energetically favourable when enough chemisorbed S atoms are present. These energetic considerations support the surface sulphidation mechanism inferred from the MD trajectories. The propagation of silver sulphide towards the inner layers proceeds in a similar fashion: when a given layer is rich in sulphur, an Ag atom moves into that layer from the one beneath, and the vacancy is filled by one S atom (Fig. S17). The Ag sulphidation mechanism is summarized in the bottom panel of Fig. 2a.

[Figure 2], [Figure 3]

Note that, for the reaction rate, the S_8 partial pressure (p_{S8}) only matters in so far as it determines the availability of S_8 molecules for the reaction, as also observed in Ref. 18. The growth of Ag_2S through upwards migration of Ag ions had been hypothesized based on experimental evidences by Wagner[19]. Our simulations confirm and provide a rationale for that model, while also extending it to the very first sulphidation stages. A similar reaction mechanism can be expected for H_2S. Once adsorbed, it will undergo deprotonation reactions, resulting in chemisorbed S atoms[18] (H_2 having been released), exactly as for S_8.

Next we analyse the role of defects. Adatoms readily bind to the adsorbed S atoms, but their presence has no sizeable effects on the reactivity of the underlying Ag layers (Fig. S16). Similarly, when steps are present on the surface, the Ag layers forming the step react faster than the defect-free surface, but the layers below are unaffected. Conversely, the presence of even a few vacancies does speed up the reaction. Adsorbed S atoms quickly fill the vacancies, making it easier for the neighbouring Ag to have S atoms close enough to promote further Ag vacancy/adatom pair formation. Finally, grain boundaries speed up the reaction considerably [see Fig. 2b]. Their effect is twofold. Their loose packing leaves more space for S penetration, and they facilitate the Ag diffusion. This latter effect is well-known in metallurgy[20]. Accordingly, the region surrounding the grain boundary is more vulnerable to sulphidation (Fig. 2b). These results support the proposed sulphidation mechanism: only those defects that favour the penetration of S atoms in the bulk and/or the migration of Ag atoms to the surface, can accelerate the tarnishing reaction.

The role of temperature, *T*, is worth discussing. In order to simulate the corrosion reactions over the timescale accessible by MD, we adopted *T*=750 K, although tarnishing is observed at ambient conditions. Simulations at lower *T* displayed a steep reaction slowdown but no changes in the reaction mechanism

(Fig. S19). Indeed, 750 K is still far from the temperature at which qualitative changes in the reactants (*e.g.* Ag melting or gas-phase molecules breaking) would take place. These evidences justify the use of high-*T* simulations for studying Ag tarnishing. The only relevant difference is that at *T*=750 K and ordinary p_{O2} , only surface (not bulk) oxidation is expected to occur[21]. Nonetheless, the rate and reaction mechanism of Ag surface oxidation can be studied through our MD simulations.

The Ag-O reactivity depends significantly on p_{O2}. At p=2 bar, no O_2 dissociation is observed within 5 ns unless the Ag surface presents grain boundaries, confirming their higher sensitivity to corrosion. At p=10 bar, a slow oxidation is observed: 7 O_2 molecules reacted in 5 ns on a 686 $Å^2$ Ag(001) surface (to be compared with 5 ns Ag-S_8 reaction on the same surface, Fig. 2c). The reaction mechanism is radically different from that of sulphidation. The physisorbed O_2 molecule *occasionally* penetrates into the first Ag layer and then dissociates within a few ps (Fig. 4). This reaction path can be rationalized from the (DFT) energetics of the relevant reaction events (Fig. 3). O_2 chemisorption becomes endothermic for moderate coverage, which suggests a high (coulombic) repulsion among adsorbed oxygen atoms. Hence, the reaction path observed for sulphidation is energetically unfavourable for the Ag-O_2 reaction. Instead, the migration of a chemisorbed O atom from a surface to a subsurface site requires an energy that is about 3 times lower than that required for sulphur (Fig. 3b). Therefore, oxygen atoms can penetrate into the Ag surface relatively easily. This fact explains the observed oxidation mechanism.

A much higher oxidation rate, and different reaction mechanisms, are observed in the MD simulations when O_2 is in supercritical conditions (p_{O2}> 50 bar) or when O_3 is present. The latter condition is of interest for in-field Ag oxidation (see introduction). Our simulations reproduce the experimentally observed high oxidizing strength[22] of O_3 and unearth the corresponding mechanism. When an O_3 molecule approaches Ag, it dissociates fast (1-10 ps) into a chemisorbed O atom, which then diffuses under the surface, and a (physisorbed) O_2 molecule (Fig. S15). The process is strongly exothermic (as seen in the TS data), and it is even faster than Ag-S_8. Overall, these results support the hypothesis that in-field, sizable Ag oxidation can only take place when ozone is present, even if this is in ppb concentrations.

[Figure 4]

We can now provide a general picture of silver tarnishing based on our simulations. Oxygen and sulphur follow different reaction mechanisms because of their different electronegativity/hardness[23] (anionic O···O repulsion is higher than S···S) and atomic size (S is bigger than O, hence cannot diffuse into Ag). The factors that make surface sulphidation much faster than oxidation were uncovered. Once an S_8 molecule approaches silver, it unavoidably binds and reacts. Instead, for O_2 we observe a low sticking coefficient, as also found experimentally[16]. More generally, O_2 molecules dissociate much more slowly than S_8, because of the kinetic barrier shown in Fig. 1. Since the probability of overcoming the barrier increases exponentially with *T* (Arrhenius' equation), we can conclude that the rate disparity between the S and O reactivity is several orders of magnitude at ambient *T*.

Having understood the mechanisms of oxidation and sulphidation, we can go one step further and sketch how the reactions can proceed over long time scales (days) at ambient p, T conditions. The

growth of Ag_2O has to proceed by O_2 dissociation at the oxide surface and O diffusion through the oxide layer towards the oxide/Ag interphase. Both processes can be expected to become slower once the Ag surface is oxidized, due to the strong O···O repulsion. Indeed, the (dissociative) sticking coefficient of O_2 was experimentally found to decrease sharply as the oxygen coverage increases[24]. As for diffusion, the repulsion hampers an interstitial mechanism. The oxygen migration is thus likely to proceed through oxygen vacancies, the dominant defects in Ag_2O[25]. Instead, MD results show the formation of silver sulphide to be relatively fast, even after the first layer has formed. The growth of the sulphide beyond the surface does not require the presence of defects (although they speed up the reaction), as the process is driven by Ag upward migration, with Ag ions being highly mobile in Ag_2S[26]. Indeed the sulphide thickness was experimentally observed to increase linearly with time upon exposure to sulphur compounds[7]. These radically different growth scenarios, combined with the time-scale difference between surface oxidation and sulphidation, explain the existence of a reactivity disparity between oxygen and sulphur in spite of their similar thermodynamics.

In conclusion, we have exploited DFT and reactive force fields to study silver tarnishing at the atomic level. Through extensive MD runs, we pinpointed the different mechanisms of silver sulphidation and oxidation thereby demonstrating why Ag is reactive to sulphur compounds but not to O_2. For this study, we developed Ag/S and Ag/O reactive force fields, whose accuracy was broadly tested. They are made available for further studies on the Ag/O/S reactivity (*e.g.* for nanoparticles) or to be adopted as a reliable starting point for studying more complex Ag-S-O-containing systems. Having unveiled the precise mechanism of silver tarnishing, we expect this work to prompt a rational materials design strategy to produce Ag-based, corrosion-resistant alloys for the electronic industry.

Acknowledgements:

This project has received funding from Science Foundation Ireland (SFI) under grant number 12/RC/2278, from the European Union's Horizon 2020 research and innovation programme under the Marie Skłodowska-Curie grant agreement No. 713567, and from the Nokia Bell Lab. Computational resources from the Trinity Center for High Performance Computing (TCHPC) are acknowledged.

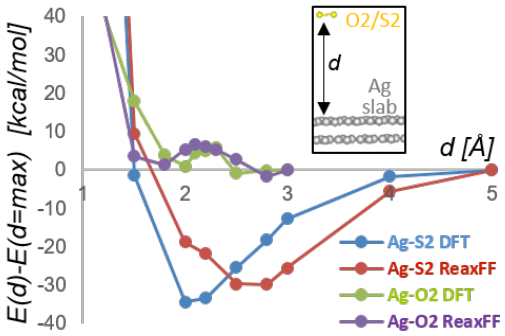

Figure 1. Energy path for O_2 and S_2 dissociation onto Ag(111). Both plane-wave DFT (VASP[27] code) and ReaxFF (lammps[28] code) values are reported. Geometry shown in the inset. The O_2/S_2 molecule is placed at different heights above the Ag surface, parallel to it, and the bond length is let free to relax. The change in energy with respect to the maximum height considered (3.0 and 5.0 Å for O_2 and S_2, respectively) is calculated. Detailed description of the system in Sect. S2.1.

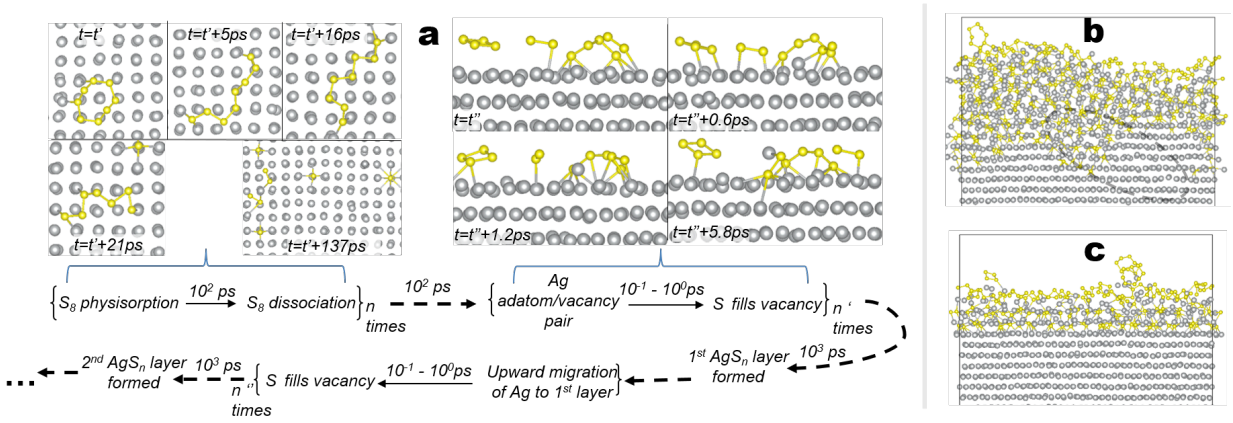

Figure 2. Ag(001) sulphidation snapshots. (a) Scheme of Ag-S reaction mechanism. Illustrative snapshots are shown. (b) and (c) are the snapshots at t=5 ns (T=750 K) in presence and absence of Σ5(310) GB, respectively. Solid lines indicate unit cell boundaries. The GB is highlighted by the dotted circle. Note the GB was built perpendicular to the surface, and it migrated during the simulation. Ag(S) atoms are drawn in grey (yellow).

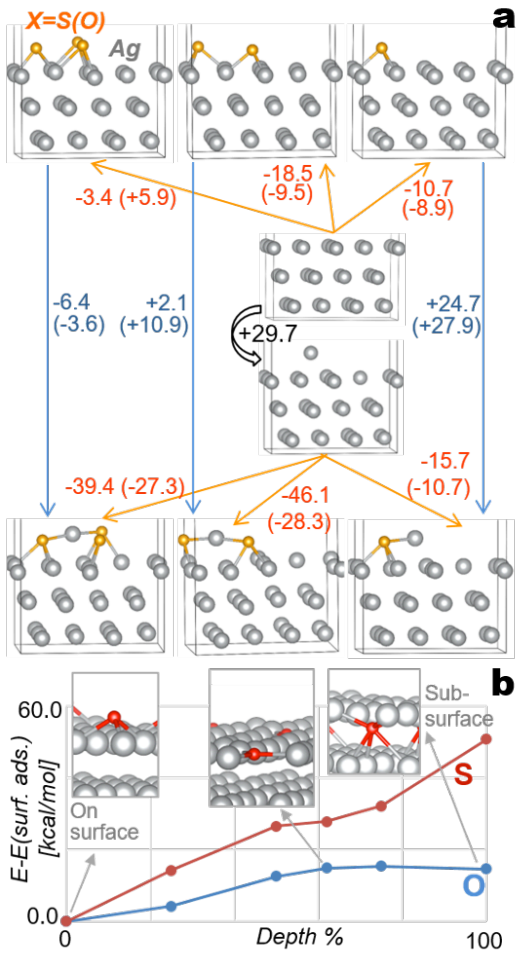

Figure 3. DFT energetics for relevant steps of Ag-S and Ag-O reactions. (a) adatom/vacancy pair formation energies (kcal/mol) on bare surface (black number) and in presence of 1,2 or 3 adsorbed atoms (blue numbers). Orange numbers/arrows indicate the chemisorption energy (as defined in ref. 10) of 1,2 or 3 O/S atoms on the bare surface (upper part) and on the surface with adatom/vacancy pair (lower part). The values out of (in) parenthesis refer to sulphur (oxygen). (b) energy profile of an S/O atom moving from the equilibrium on-surface to sub-surface position. The depth is defined as the relative position of the O/S atom along the path connecting on-surface to sub-surface sites, in percentage. Calculation details in Sect. S1.1.

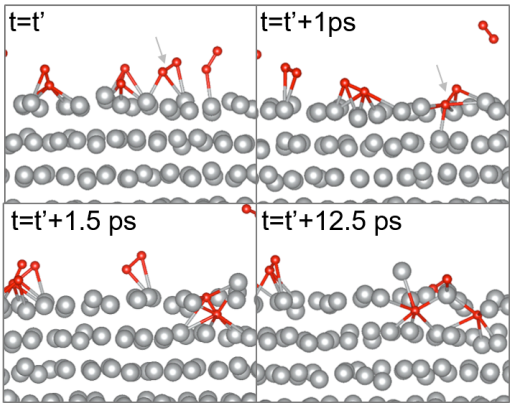

Figure 4. MD snapshots showing the mechanism of O_2 dissociation and penetration to Ag surface. The grey arrow indicates the molecule that is going to react (O atoms in red).

REFERENCES

[1] S. Zhang, Y. Tang, B. Vlahovic, *Nanoscale Research Letters* **2016**, *11*, 80.
[2] M. Arra, D. Shangguan, D. Xie, J. Sundelin, T. Lepistö, E. Ristolainen, *Journal of Elec Materi* **2004**, *33*, 977–990.
[3] M. Scuderi, M. Esposito, F. Todisco, D. Simeone, I. Tarantini, L. De Marco, M. De Giorgi, G. Nicotra, L. Carbone, D. Sanvitto, et al., *J. Phys. Chem. C* **2016**, *120*, 24314–24323.
[4] R. Schueller, *SMTA News and Journal of Surface Mount Technology* **2008**, *21*, 21.
[5] J. P. Franey, G. W. Kammlott, T. E. Graedel, *Corrosion Science* **1985**, *25*, 133–143.
[6] R. Wiesinger, I. Martina, C. Kleber, M. Schreiner, *Corrosion Science* **2013**, *77*, 69–76.
[7] B. T. Reagor, J. D. Sinclair, *J. Electrochem. Soc.* **1981**, *128*, 701–705.
[8] C. E. Sanders, D. Verreault, G. S. Frankel, H. C. Allen, *J. Electrochem. Soc.* **2015**, *162*, C630–C637.
[9] P. Patnaik, *Handbook of Inorganic Chemicals*, McGraw-Hill Professional, New York, **2002**.
[10] G. Saleh, C. Xu, S. Sanvito, *Phys. Chem. Chem. Phys.* **2018**, *20*, 4277–4286.
[11] V. Maurice, P. Marcus, *Electrochimica Acta* **2012**, *84*, 129–138.
[12] A. C. T. van Duin, S. Dasgupta, F. Lorant, W. A. Goddard, *J. Phys. Chem. A* **2001**, *105*, 9396–9409.
[13] K. Chenoweth, A. C. T. van Duin, W. A. Goddard, *J. Phys. Chem. A* **2008**, *112*, 1040–1053.
[14] B. Jeon, S. K. R. S. Sankaranarayanan, A. C. T. van Duin, S. Ramanathan, *ACS Appl. Mater. Interfaces* **2012**, *4*, 1225–1232.
[15] R. Subbaraman, S. A. Deshmukh, S. K. R. S. Sankaranarayanan, *J. Phys. Chem. C* **2013**, *117*, 5195–5207.
[16] F. Besenbacher, J. K. Nørskov, *Progress in Surface Science* **1993**, *44*, 5–66.
[17] L. Vitos, A. V. Ruban, H. L. Skriver, J. Kollár, *Surface Science* **1998**, *411*, 186–202.
[18] T. E. Graedel, J. P. Franey, G. J. Gualtieri, G. W. Kammlott, D. L. Malm, *Corrosion Science* **1985**, *25*, 1163–1180.
[19] C. Wagner, *Zeitschrift für Physikalische Chemie* **1933**, *21B*, 25–41.
[20] R. W. Balluffi, *JEM* **1992**, *21*, 527–553.
[21] T. E. Jones, T. C. R. Rocha, A. Knop-Gericke, C. Stampfl, R. Schlögl, S. Piccinin, *Phys. Chem. Chem. Phys.* **2015**, *17*, 9288–9312.
[22] G. I. N. Waterhouse, G. A. Bowmaker, J. B. Metson, *Applied Surface Science* **2001**, *183*, 191–204.
[23] N. Islam, D. C. Ghosh, *Journal of Quantum Information Science* **2011**, *01*, 135.
[24] L. Vattuone, M. Rocca, C. Boragno, U. Valbusa, *J. Chem. Phys.* **1994**, *101*, 726–730.
[25] A. Wöhnke, R. Haul, H. Schmalzried, *Zeitschrift für Physikalische Chemie* **1994**, *186*, 215–226.
[26] I. Bartkowicz, S. Mrowec, *physica status solidi (b)* **1972**, *49*, 101–105.
[27] G. Kresse, J. Furthmüller, *Computational Materials Science* **1996**, *6*, 15–50.
[28] S. Plimpton, *Journal of Computational Physics* **1995**, *117*, 1–19.